

A two-layer model of the ionosphere using Global Positioning System data

J.Miguel Juan

Dept. Física Aplicada, UPC, c/Gran Capità s/n., 08034 Barcelona, Spain

Antonio Rius

Institut d'Estudis Espacials de Catalunya (IEEC-CSIC), c/Gran Capità 2-4, 08034 Barcelona, Spain

Manuel Hernández-Pajares and Jaume Sanz

Dept. Matemàtica Aplicada i Telemàtica, UPC, c/Gran Capità s/n. 08034 Barcelona, Spain

Abstract. We present a new approach to model the Ionosphere based on GPS data. Previous authors have used models with an unique shell. In this case we have included a second shell to account for the distribution of the electrons in the outer part of the Ionosphere. We have analyzed the ionospheric electron content of a region above 30 degrees in declination in different conditions of ionospheric activity using the Kalman filter. The data used has been obtained from the *International GPS Service for Geodynamics* (IGS) network. Simultaneously we have studied the receiver and transmitter differential biases showing the effects of neglecting the outer part of the Ionosphere in the model. It appears a systematic variations for the receivers—depending on its latitude—not for the satellites.

Introduction

It has been shown that the Global Positioning System (GPS) is a useful tool to estimate the ionospheric Total Electron Content (TEC) (see, for instance, *Lanyi and Roth 1988, Sardón et al., 1994, Manucci et al., 1993*). In these works the Ionosphere is treated as one shell, with an approximate height of around 350 km, where all the electrons are confined, and consequently no ionospheric delay occurs outside it. *Klobuchar et al., [1994]* (see also *Klobuchar et al., 1995*) have pointed out that these models do not include the contribution of the electrons in the outer shells, like the *protonosphere*. In fact the electron density is typically 2 orders of magnitude lower in the external shells but the GPS signal paths are mainly included there. In order to take into account these effects we have developed a two-layered model.

Model

We will concentrate our study on the effects of the ionosphere—a dispersive medium—on the phase and group delay of this media, Δs_k^g and Δs_k respectively. As is well known (see for instance *Davies 1990, page 73*), Δs_k^g , $\Delta s_k(m)$, are related with the *slant TEC I* (in electrons/ m^2) and the frequency of the signal f_k (in Hz), through the formulae:

$$\Delta s_k^g = -\Delta s_k \simeq \alpha_k I \quad (1)$$

where $\alpha_k = \frac{40.3}{f_k^2}$.

Each GPS satellite i transmit two signals L1 ($f_1 \sim 1.6$ GHz) and L2 ($f_2 \sim 1.2$ GHz), which are processed at the GPS receiver j producing time tagged values of their group and phase delays: $P_{ki}^j(t)$ and $L_{ki}^j(t)$ at the frequency f_k . After detecting and correcting the *cycle-slips* of the phases $L_{ki}^j(t)$ using the group delays $P_{ki}^j(t)$, we get the corrected phases \hat{L}_{ki}^j (see *Blewitt 1990*). The difference between these two corrected phases—named *ionospheric combination*—depends only on the ionospheric differential delay between the two frequencies, jointly with the instrumental delays:

$$\hat{L}_{1i}^j - \hat{L}_{2i}^j = \Delta s_1 - \Delta s_2 + K_i + K^j \quad (2)$$

Finally, applying 1 to 2, we obtain the relationship 3.

$$\hat{L}_{1i}^j - \hat{L}_{2i}^j = (\alpha_2 - \alpha_1)I + K_i + K^j \quad (3)$$

where K_i, K^j are constants associated to the frequency dependent delays of station i and satellite j . We consider as errors the contributions associated to multipath phenomena, to the antenna phase center mismodelling (*Shupler et al., 1994*) and to the scattering effects (*Elosegui et al., 1995*).

This equation can be rewritten in terms of the electronic density n_e , using the standard tomographic notation (see, for instance, *Nolet 1987*) and defining $n = (\alpha_2 - \alpha_1)n_e$:

$$\hat{L}_{1i}^j - \hat{L}_{2i}^j = \int_{\mathfrak{R}_i^j} n dx + K_i + K^j = \int_{\mathfrak{R}_i^j} \frac{1}{\cos X} n dr + K_i + K^j \quad (4)$$

dx being the length element of the ray \mathfrak{R}_i^j between the satellite j and receiver i , dr the corresponding geocentric radial element and X is the angle between the given ray and the geocentric radial direction; $\frac{1}{\cos X}$ is known as the *mapping function* for the layer $[r, r + dr]$. The situation is in fact more complex than in the standard computer aided tomography (Raymund 1994). For the same reasons as those described in Bevis *et al.*, 1992 we should refer to the present application as *ionospheric stochastic tomography*.

Our purpose is to use Eq. 4 to obtain n with observations from receivers placed on the Earth crust. Because the mapping function tends to be constant when r increases, the ionospheric delay corresponding to outer shells tends to present signatures close to those of the instrumental delays. Consequently, we have limited the integration interval in Eq. 4 to a height of 5000 km. The main effect of this assumption is to bias the estimated instrumental constants.

In order to estimate the electron density and the instrumental delays, we can discretize Eq. 4 using spherical geocentric layers. Each spherical geocentric layer is divided into a certain number of cells:

$$\hat{L}_{1i}^j - \hat{L}_{2i}^j = \sum_{k=1}^N \sum_{c_k=1}^{N_k} n_{k,c_k}(t) \Delta x_i^j(k, c_k) + K_i + K^j + \epsilon \quad (5)$$

where N is the number of layers, and each layer k is divided in N_k cells; $\Delta x_i^j(k, c_k)$ is the length of the part of the ray included in the cell c_k ; ϵ is the noise term mainly due to the discretization error. Because the number of cells crossed by a particular ray is relatively small, the matrix representation of Eq. 5 will be sparse. The radial total electron content (TEC) T_{k,c_k} of the cell c_k could be obtained as:

$$T_{k,c_k} = n_{k,c_k} \cdot h_k \quad (6)$$

where h_k is the thickness of the layer k .

Data Analysis

As an application of this approach we use two models that will be compared: the first one with one spherical layer limited by heights 50 and 500 km; the second with two spherical layers with limits at heights 50, 500 and 5000 km. Each shell has been divided into cells of 10×10 degrees, and the integration time has been taken as 6 hours.

The coordinate system chosen is the *Equatorial Geocentric* reference system: the X axis points towards the Vernal equinox, the Z-axis towards the North astronomical Pole and the Y-axis forms a positive oriented reference frame. We use the typical associated spherical coordinates: geocentric distance, right ascension (RA) and declination (DEC).

In this reference system the Sun only changes 1 degree per day approximately (so it is quasi-fixed); and the North magnetic pole differs around 12 degrees from the Z-axis. Therefore with these coordinates the description of the ionosphere can be assumed more stationary than in others commonly used (i.e. longitude-latitude).

Each solution obtained after analyzing 6 hours of data has been recursively combined using a Kalman filter. We assume that the TEC variations between consecutive solutions are modeled as a random walk with a process noise in 6 hours of $\sigma_{6h} = 10$ cm and the instrumental delays are considered constants.

To solve the problem of cells poorly illuminated, in the present analysis we have weakly constrained the electron content of each cell to be the TEC mean extended over all the neighbouring cells. Then:

$$T_{k,c_k} - \bar{T}_{k,c_k} = 0 \quad (7)$$

where \bar{T}_{k,c_k} is the mean TEC value computed in the neighborhood of cell c_k .

With only ground data there are not enough information about vertical structures (Hajj *et al.*, 1994), so we have constrained the value of the polar cells (DEC=90) to zero.

We have used dual GPS frequency data collected at 30 IGS sites with latitudes greater than 20 degrees dur-

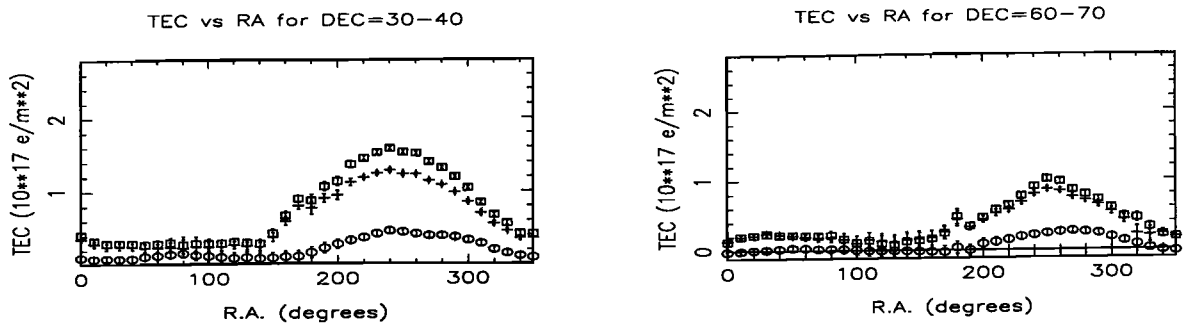


Figure 1. In each box we have plotted the TEC corresponding to 24:00 UT 17 November 1993 for the shells contained in the indicated declination interval as a function of the right ascension of the cell. The crosses are corresponding to the 1st shell and the circles to the 2nd shell. Also, as a reference, we have included the corresponding TEC obtained with the one-shell model (squares). Each symbol has associated its 1-sigma error bars.

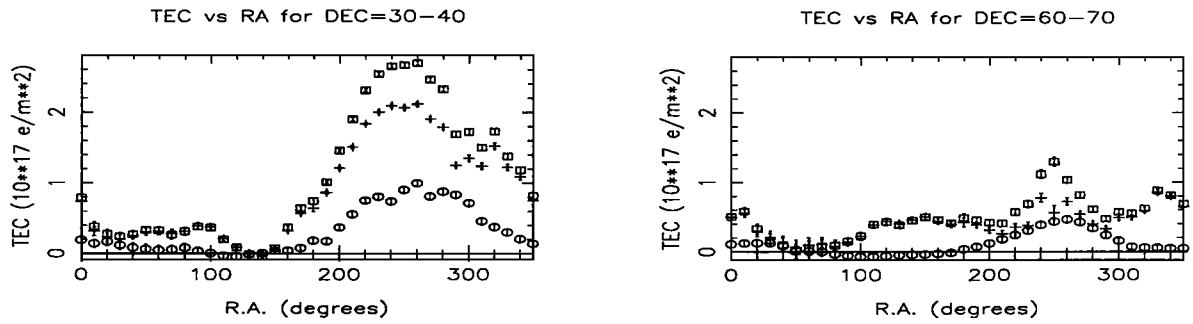


Figure 2. Equivalent plots than those of Fig. 1, for the day 18 November 1993, 18:00 UT which presents high geomagnetic activity.

ing the period 15-19 November 1993. In order to avoid estimating TEC for cells crossed by a few rays, we have rejected the rays crossing the first layer with declinations lower than 30 degrees, where the IGS station distribution is sparse. During this period there was an important increase in geomagnetic activity, especially at 18-Nov ~12 hours. At this epoch the "Planetary Equivalent Amplitude Index" collected by the US National Geophysical Data Center increased by a factor of 10.

Results

As an example of our computations we present in Figures 1 and 2 the radial TEC for the days 17 at 24:00 and 18 November 1993 at 18:00, respectively. The approximate Sun coordinates were RA=230 degrees and DEC=-18 degrees. The most interesting features are:

- The results for the geomagnetic quiet day 17 November 1993 are smoother and smaller than the corresponding results for the geomagnetic active day 18.
- TEC values for the second layer is detected and is related with the Sun direction (RA =230 degrees, DEC=-18 degrees) .
- In general we get the following relationships:

$$T_1 < T^{single} < T_1 + T_2 \tag{8}$$

where T_1, T_2 are the corresponding TECs for the first and second layer, and T^{single} is the value obtained modelling only the first layer.

- The relative contribution T_2/T_1 between the two shells are in general larger for the active geomagnetic day.
- For the two days we get root mean squared (RMS) of < 10 cm with the two-layer model, better than the RMS obtained with one-layer models (≈ 20 cm in our case and in the model of Wilson et al. (1995))

Regarding the instrumental delay estimation:

For stations: In figure 3 we have represented the difference of station estimated delays $DK_i = K_i -$

K_i^{single} as a function of the station latitude. The observed trend (dashed line in the figure) is explained, for declinations greater than 30 degrees, in terms of the presence of the 2nd layer TEC which depends on the declination difference between the total TEC for the two shells minus the single shell TEC (see equation 8).

For satellites: There are not systematic trend between the 1 and 2-layer models. The mean difference is 0.01 with an rms of 0.01 ns. The results obtained are also in agreement for the common satellites with those values ftp-published by the DLR/DFD of Neustrelitz (Germany) at the end of June 1995 with a difference rms of 0.2 ns ($\approx 0.6 \times 10^{16} e/m^2$). It should be remarked that both sets of constants were obtained with data taken at different epochs, fixing to zero the same station delay.

Conclusions and Discussion

The total electron content of the Ionosphere produces delays in EM signals crossing it. Neglecting its 3-D

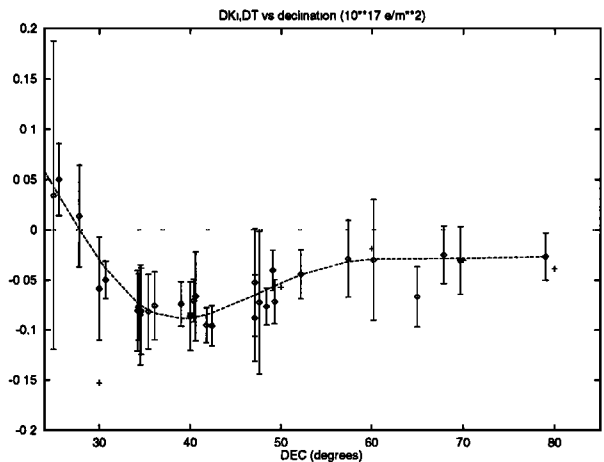


Figure 3. In this figure it is plotted the difference of the station instrumental delays computed with two shells minus those computed with one shell as a function of the station zenith declination (latitude) –diamonds with error bars–. The dashed line is a spline approximation to these results.

structure has been a limitation of previous uses of the GPS data for measuring the TEC. In the present paper we have used a 2-layer model to study the TEC with a stochastic tomographic approach. We have been able to characterize with low resolution the time varying 3-D structure of the TEC on a global scale.

In order to do so, we have chosen alternative coordinates—right ascension and declination—which present some advantages: (1) The ionosphere can be considered stationary within a certain time interval. (2) Allows a global study of the ionosphere mixing rays for different pairs station-satellite. (3) Provide a common reference system to compare estimation during different epochs.

Also, we have revisited the problem of the determination of the receiver and satellite differential biases doing a comparison between their estimations obtained using 1 and 2 layers. While for the satellite constants we have found an agreement at a level of 0.01 ns between the one and two layer models, for the receiver constant we have found systematic differences as a function of the latitude of the station. This difference could be explained in terms of the different geometry of the station and satellite paths. Notice that the station instrumental delays are mainly estimated from data with similar declinations, i.e. collected at similar latitudes. This is not the case for the satellites.

Finally, we can comment that the discretization errors could be important considering only two layers. Nevertheless these errors are, common to the first layer in both models, and very small for the low electron density of the second layer. So this not affects to the delay comparison study.

Acknowledgments

This work was supported in part by the projects *DGI-CYT* Nbrs. PB93-1235 and PB94-1205.

References

- Bevis M., Businger S., Herring T.A., Rocken C., Anthes R.A., Randolph H.W., 1992. GPS Meteorology: Remote Sensing of Atmospheric Water Vapour using the Global Positioning System. *Journal of Geophysical Research*, Vol.97, No. D14, 15787-15801.
- Blewitt G., 1990. An automatic editing algorithm for GPS data. *Geophysical Research Letters*, Vol.17, No.3, pages 199-202.
- Davies K., 1990. *Ionospheric Radio*. IEE ElectroMagnetic Waves Series 31, Peter Perigrinus Ltd., London.
- Elosegui P., Davis J.L., Jaldehag R.T.K., Johansson J.M., Neill A.E. Niell, Shapiro I.I., 1995. Geodesy using the Global Positioning System: The effects of signal scattering on estimates of site position. *Journal of Geophysical Research*, Vol 100, No. B7, pp9921-9934, June 10
- Freymueller J.T., 1993. PhasEdit version 1.1: An automatic data editing program for dual-frequency codeless GPS receivers. An Introduction to GIPSY/OASIS-II, eds. F.H. Webb & J.F. Zumberge, JPL.
- Haji G.A., Ibañez-Meier R., Kursinski E.R., Romans L.J., 1994. Imaging the Ionosphere with the Global Positioning System. *Imaging Systems and Technology*, Vol.5, 174-184.
- Klobuchar J.A., Doherty P.H., Bailey G.J., Davies K., 1994. Limitations in Determining Absolute Total Electron Content from Dual-Frequency GPS Group Delay Measurements. Beacon Satellite Symposium, Aberystwyth, July 11-15 1994.
- Klobuchar J.A., Doherty P.H., Barkry M., Conker R.S., 1995. Correcting for the Effects of Ionospheric Range Delays on the Proposed Wide-Area Augmentation System (WAAS). 1995 Spring Meeting of the American Geophysical Union, Eos supplement, Vol.76, No.17.
- Lanyi, G.E., Roth, T., 1988. A comparison of mapped and measured total ionospheric electron content using Global Positioning System and beacon satellite observations. *Radio Science*, Vol.23, No.4, 483-492.
- Mannucci A., Wilson B., Edwards C., 1993. A New Method for Monitoring the Earth's Ionospheric Total Electron Content using the GPS global network. ION GPS-93, Salt Lake City, Utah.
- Nolet G., 1987. *Seismic tomography with applications in Global Seismology and Exploration Geophysics*, D.Reidel Publishing Company.
- Raymund. T.D., 1994. Ionospheric Tomography Algorithms. *International Journal of Imaging Systems and Technology*, Vol. 5, 75-85.
- Sardon E., Rius, A., Zarraoa N., 1994. Estimation of the transmitter and receiver differential biases and the ionospheric total electron content from Global Positioning System observations. *Radio Science*, Vol.29, No.3, pages 577-586.
- Schupler B.R., Allshouse R.L., Clark T.A., 1994. Signal characteristics of GPS user antennas. *Navigation*, 41, 277-295.
- Wilson B.B., Mannucci A.J., Edwards C.B., 1995. Subdaily northern hemisphere ionospheric maps using an extensive network of GPS receivers. *Radio Science*, 30, 639-648.
- Zumberge J., Neilan R., Beutler G., Gurtner W., 1994. The International GPS Service for Geodynamics-Benefits to Users. ION GPS-94, Salt Lake City, Utah.

(Received September 19, 1996; revised December 12, 1996; accepted December 12, 1996.)